Powder Metallurgy and Metal Ceramics, Vol. 47, Nos. 5-6, 2008

THERMODYNAMIC ASSESSMENT OF THE Cu–Ti–Zr SYSTEM. I. Cu–Ti SYSTEM

M. A. Turchanin,[1,2] P. G. Agraval,[1] and A. R. Abdulov[1]

UDC 669.5.017.11:546.56′82

The CALPHAD method is used for the thermodynamic assessment of the Cu–Ti system that bounds the ternary Cu–Ti–Zr system, which is capable of forming amorphous alloys. The self-consistent parameters of thermodynamic models of the phases are obtained from data on the phase equilibria and thermodynamic properties of liquid alloys and intermetallic compounds. The Gibbs energy of the liquid phase is described using the associated ideal solution model. To describe the thermodynamic properties of the Cu_4Ti and CuTi intermetallic compounds with homogeneity range, sublattice models are used. The calculated phase diagram of the system and the thermodynamic properties of the phases are in good agreement with experimental data.

Keywords: *phase diagram, thermodynamics, thermodynamic modeling, copper–titanium alloys.*

INTRODUCTION

The interest in metal systems that are prone to form amorphous alloys under nonequilibrium synthesis conditions is due to their unique mechanical (hardness, strength, plasticity), chemical (corrosion resistance, gas-absorbing ability), magnetic, and electric properties. Most amorphous alloys were obtained by melt-quenching at cooling rates from 10^5 to 10^6 K/sec. Therefore, this involved many technological difficulties, and fast-quenched amorphous alloys could only be obtained in the form of thin ribbons, flakes, filaments, or powders. The new family of amorphous alloys based on multicomponent systems, such as Cu–Ti–Zr, exhibits extraordinary susceptibility to amorphization. This makes it possible to obtain amorphous compositions at low cooling rates ($1–10^2$ K/sec) close to the traditional foundry conditions. Alloys of this family are called bulk amorphous alloys.

Though the possibility of developing new compositions of fast-quenched and bulk amorphous alloys appears promising, there are still few such systems and compositions [1, 2] because there has been no systematic theoretical study of the phenomenon. Since the discovery of amorphous alloys, emphasis has been placed on the development of new dot-like multicomponent compositions. While the mechanical and some other physical properties of such alloys have generally been studied, their thermodynamic properties as well as the thermodynamic properties of their melts are yet to be understood. It is currently impossible to compare the thermodynamic stability of the phases that compete during amorphization because no data are available on the thermodynamic properties of equilibrium and supercooled melts in the corresponding systems. Therefore, the phenomenon cannot be described quantitatively and the factors that affect it cannot be identified. In this regard, the Cu–Ti–Zr system is suitable for the theoretical treatment of the processes used to produce fast-quenched and bulk amorphous alloys. The phase

[1]Donbass State Mechanical Engineering Academy, Kramatorsk, Ukraine.
[2]To whom correspondence should be addressed; e-mail: turch@dgma.donetsk.ua.

Translated from Poroshkovaya Metallurgiya, Vol. 47, No. 3–4 (460), pp. 102–121, 2008. Original article submitted December 20, 2007.

 1068-1302/08/0506-0344

transformations in this system were experimentally studied in [3–7] for equilibrium alloys and in [8–10] for amorphous alloys. The data on equilibrium phase transformations obtained in [4, 5] were used, together with the CALPHAD method, in [11] for the thermodynamic assessment of the system. The merits and demerits of the results obtained in [11] were detailed in [12]. New experimental data on the mixing enthalpy of Cu–Ti–Zr melts [13], phase transformations in the system [7], the mixing enthalpy of Ti–Zr melts [14], and the temperature dependence of the integral mixing enthalpy of Cu–Ti [15] and Cu–Zr [16] melts provide the basis for new thermodynamic assessment.

DATA ON PHASE TRANSFORMATIONS AND THERMODYNAMIC PROPERTIES OF THE PHASES

Phase Transformations. Stable phase transformations in the Cu–Ti system have long been the subject of numerous research efforts [17–37], which are reviewed in Table 1 and whose results are presented in Figs. 1–4. The coordinates of invariant equilibria obtained by different authors are systematized in Table 2. The results obtained until 1983 were detailed in [38].

The liquidus of the (Cu)-phase (Fig. 1) was studied in [18–20, 26, 27]. The data obtained in [20, 26, 27] are in good agreement and indicative of the flatness of this liquidus line. The results of [18, 19] correspond to higher temperatures. Note that in the range $x_{Ti} = 0.2–0.5$ the liquidus data obtained in [20, 26, 27] are also in good agreement, whereas the data of [18, 19] regularly deviate from them. Therefore, the data from [18, 19] will be ignored below in describing the liquidus of the (Cu)-phase as well as other sections of the liquidus in the range $x_{Ti} = 0.2–0.5$. The region of the (Cu)-phase (Fig. 1) was studied in [19–23, 30, 31, 36]. Comparing data on the solubility of titanium in copper, we favor those obtained in [20–23, 36].

According to the experimental data [3, 18–20, 24–28, 31–35, 37, 39–41], a number of intermetallic compounds form in the system. In [18–20, 25, 39], the copper-richest intermetallic compound was assumed to be Cu_3Ti. It was established in [39] that this compound forms in the concentration range $x_{Ti} = 0.21–0.25$. It is Cu_4Ti according to [26–28, 31]. It was revealed in [26, 27] that this compound is homogeneous in the range $x_{Ti} = 0.20–0.22$. According to [28], Cu_4Ti with $x_{Ti} = 0.191$ is in equilibrium with the (Cu)-phase. In [31], it was discovered that the alloys are one-phase in the range $x_{Ti} = 0.202–0.216$. Analyzing experimental data on the region of the Cu_4Ti phase (Fig. 1), we favored the information from [27, 28, 31]. It is pointed out in [31] that there are two modifications of Cu_4Ti between which peritectoid transformation occurs at 773 K. Since this information was not supported by other authors, we will not take it into account.

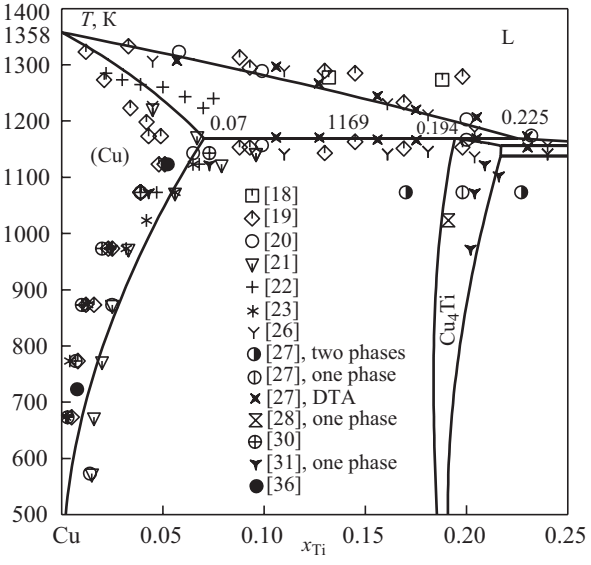

Fig. 1. Experimental and theoretical phase boundaries for (Cu)-phases and Cu_4Ti: here and later on, symbols stand for experimental data and lines for calculated results

TABLE 1. Review of Experimental Studies on the Stable Phase Equilibria in the Cu–Ti System

Reference	Method	Phase diagram region analyzed
[17]	Heterogeneous equilibrium	T = 1023–1173 K, x_{Ti} = 0.95–1; (βTi)/((αTi) + (βTi)), (αTi)/((αTi) + (βTi))
[18]	Thermal and x-ray analyses, metallography	T = 873–1373 K, x_{Ti} = 0.18–1; liquidus (Cu), Cu_4Ti, Cu_3Ti_2, and CuTi phases; (βTi)/($CuTi_2$ + (βTi)), (βTi)/((αTi) + (βTi)), (αTi)/((αTi) + (βTi)), (αTi)/($CuTi_2$ + (βTi))
[19]	Ditto	T = 673–1333 K, x_{Ti} = 0–0.7; liquidus (Cu), Cu_4Ti and CuTi phases; (Cu)/((Cu) + L), (Cu)/((Cu) + Cu_4Ti)
[20]	«	T = 573–1373 K, x_{Ti} = 0–0.75; liquidus (Cu), Cu_4Ti, Cu_2Ti, Cu_3Ti_2, CuTi, and $CuTi_2$ phases; (Cu)/((Cu) + Cu_4Ti)
[21]	Thermal analyses, metallography, microhardness testing	T = 573–1223 K, x_{Ti} = 0–0.25; (Cu)/((Cu) + L), (Cu)/((Cu) + Cu_4Ti)
[22]	Metallography	T = 873–1273 K, x_{Ti} = 0–0.067; (Cu)/((Cu) + L); solubility of Ti in (Cu)-phase
[23]	Microhardness and resistance testing	T = 573–1123 K, x_{Ti} = 0–0.065; solubility Ti in (Cu)-phase
[24]	X-ray and X-ray microspectrum analyses, metallography	x_{Ti} = 0.05–0.55; invariant transformations with Cu_4Ti, Cu_2Ti, Cu_4Ti_3, and CuTi
[25]	X-ray analysis	x_{Ti} = 0.25–0.5; crystalline Cu_4Ti, Cu_2Ti, Cu_3Ti_2, and CuTi
[26]	Thermal and x-ray analyses, metallography	T = 1073–1356 K, x_{Ti} = 0–0.8; liquidus (Cu), Cu_4Ti, Cu_2Ti, Cu_3Ti_2, Cu_4Ti_3, CuTi, and $CuTi_2$; (Cu)/((Cu) + L)
[27]	Thermal and x-ray analyses, metallography	T = 1073–1356 K, x_{Ti} = 0–0.8; liquidus (Cu), Cu_4Ti, Cu_2Ti, Cu_3Ti_2, Cu_4Ti_3, CuTi, and $CuTi_2$
[28]	Electron microscopy	T = 1023 K, x_{Ti} = 0.057; Cu_4Ti structure
[29]	Thermo-emf measurement	T = 748–1048 K; solubility of Cu in (αTi)
[30]	X-ray analysis, microhardness and resistance testing	T = 443–1143 K, x_{Ti} = 0–0.073; solubility of Ti in (Cu)-phase
[31]	Metallography, X-ray analysis, resistance testing	T = 673–1223 K, x_{Ti} = 0–0.21; solubility of Ti in (Cu)-phase; Cu_4Ti homogeneity range
[32]	Differential thermal analysis, metallography, X-ray analysis	T = 1100–1357 K, x_{Ti} = 0.48–0.52; T_m^{CuTi}, phase transformations with CuTi
[33]	Thermal and x-ray analyses, X-ray microspectrum analysis, metallography	T = 1223–1373 K, x_{Ti} = 0.67; melting temperature of $CuTi_2$
[34]	Scanning electron microscopy, X-ray microspectrum analysis	T = 1023–1373 K, x_{Ti} = 0.66–1.0; (βTi)/(L + (βTi)), (βTi)/($CuTi_2$ + (βTi)), (βTi)/((αTi) + (βTi)), (αTi)/((αTi) + (βTi)), (αTi)/($CuTi_2$ + (βTi))
[35]	Metallography, scanning electron microscopy, X-ray microspectrum analysis	T = 1123 ±10 K, x_{Ti} = 0–1; Cu_4Ti, Cu_2Ti, Cu_3Ti_2, CuTi, and $CuTi_2$
[36]	X-ray analysis	T = 723, 1173 K, x_{Ti} = 0.02–0.07; solubility of Ti in (Cu)-phase
[37]	Differential thermal analysis, electron microscopy, X-ray analysis	T = 293–1373 K; x_{Ti} = 0.725–0.8; transformations with $CuTi_3$

Comment. In [18–21, 25], Cu_3Ti was used instead of Cu_4Ti.

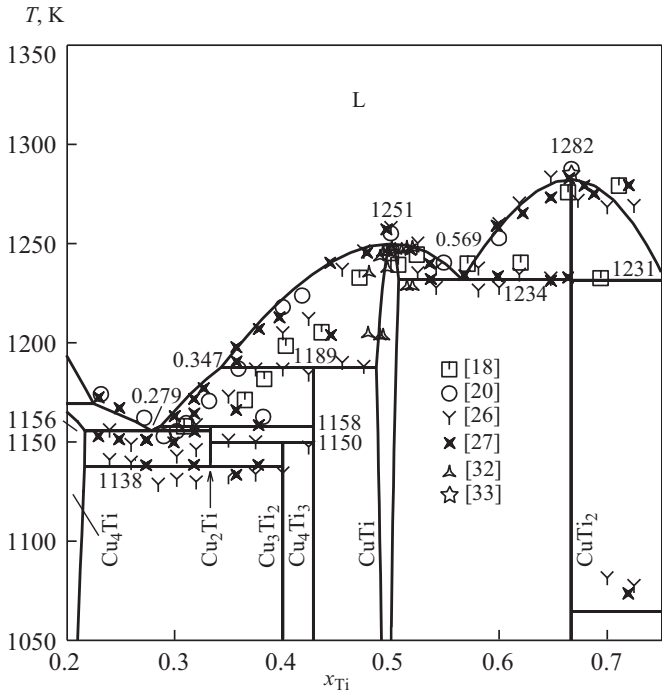

Fig. 2. Experimental and theoretical phase boundaries for intermetallic compounds of the copper–titanium system

The liquidus line in the concentration range where the intermetallic compounds Cu_2Ti, Cu_3Ti_2, Cu_4Ti_3, CuTi, and $CuTi_2$ exist (Fig. 2) was examined in [18, 20, 26, 27, 32, 33]. In [25–27], the phases Cu_2Ti, Cu_3Ti_2, and Cu_4Ti_3 were experimentally discovered in the range $x_{Ti} = 0.25–0.45$. Generalizing these studies, we conclude that the intermetallic compounds do not have homogeneity ranges.

The compound Cu_4Ti_3 forms at a temperature higher than 1200 K according to [20, 27] and at 1190 K according to [18, 26].

It is pointed out in [19, 39] that there are two phases in CuTi: one with excess copper and the other with excess titanium. The concentration range for the CuTi phase is $x_{Ti} = 0.45–0.53$. It was later established in [26, 27] that the system has only one phase CuTi with a tetragonal *B11*-type lattice and the homogeneity range $x_{Ti} = 0.48–0.52$ at $T \le 1173$ K [26] and $x_{Ti} = 0.50–0.52$ at 1073 K [27]. In [32], it was discovered that annealed alloys are single-phase in a narrower range ($x_{Ti} = 0.495–0.506$). According to the differential thermal analysis (DTA) [32], the polymorphic transformation of the CuTi phase can occur at 1190–1205 K. In modeling the CuTi phase, we used the homogeneity range of this compound established in [32]. The polymorphic transformation of CuTi cannot be described, according to [32], because of the lack of data for constructing thermodynamic models.

That $CuTi_2$ exists was established in [3, 18, 26, 27, 33, 40]. This compound is stoichiometric according to [3, 18, 40], and its homogeneity range is $x_{Ti} = 0.67–0.70$ according to [26, 27]. Agreeing with [38], we favor the results of [3, 18, 40] and consider the $CuTi_2$ phase to be stoichiometric. The $CuTi_2$ compound forms in the peritectic reaction L + (βTi) ⇔ $CuTi_2$ according to [18] and in the eutectic reaction L ⇔ $CuTi_2$ + (βTi) according to [20, 26, 27, 33]. In [20, 26, 27, 33], this compound is considered congruently melting (Fig. 4, Table 2).

There still remains the disputable question of whether $CuTi_3$ can form in an equilibrium system. That this compound exists was established in [37, 39, 41]. According to [37], the reaction $CuTi_2$ + (βTi) ⇔ $CuTi_3$ occurs at 1163 K. However, it was shown in [37] that $CuTi_2$ forms instead of CuTi in slow-quenched samples (cooling rate 5 K/min). Therefore, we may say that the $CuTi_3$ compound does not form in equilibrium conditions.

TABLE 2. Coordinates of Invariant Equilibria in the Cu–Ti System

$L + (Cu) \Leftrightarrow Cu_4Ti$

T, K	x_{Ti}^{L}	$x_{Ti}^{(Cu)}$	$x_{Ti}^{Cu_4Ti}$	Reference
		Experimental data		
1158	–	0.056	0.25	[18]
1163	0.33	0.063	0.20–0.25	[19]
–	0.230 ± 0,01	–	0.25	[24]
1143	–	–	0.20–0.22	[26]
1165 ± 3	–	–	0.20–0.22	[27]
>1123	–	>0.073	0.207–0.215	[31]
		Calculated data		
1169	0.208	0.079	0.192	[47]
1169	0.225	0.070	0.194	P. p.*

$L \Leftrightarrow Cu_4Ti + Cu_2Ti$

T, K	x_{Ti}^{L}	$x_{Ti}^{Cu_4Ti}$	$x_{Ti}^{Cu_2Ti}$	Reference
		Experimental data		
1146	0.34	0.2–0.25	0.333	[18]
1148	–	–	–	[19]
1153	0.29	0.25	0.333	[20]
	0.270 ± 0.01	0.25	0.333	[24]
1133	0.27	0.2–0.22	0.333	[26]
1151	0.27	0.2–0.22	0.333	[27]
		Calculated data		
1158	0.265	0.214	0.333	[47]
1156	0.279	0.217	0.333	P. p.

$Cu_2Ti \Leftrightarrow Cu_4Ti + Cu_3Ti_2$

T, K	$x_{Ti}^{Cu_2Ti}$	$x_{Ti}^{Cu_4Ti}$	$x_{Ti}^{Cu_3Ti_2}$	Reference
		Experimental data		
1145	0.333	–	–	[20]
>1133 ± 10	0.333	0.2–0.25	0.4	[25]
1123	0.333	0.2–0.22	0.4	[26]
1138 ± 3	0.333	0.2–0.22	0.4	[27]
		Calculated data		
1142	0.333	0.213	0.400	[47]
1138	0.333	0.217	0.400	P. p.

$L + Cu_4Ti_3 \Leftrightarrow Cu_2Ti$

T, K	x_{Ti}^{L}	$x_{Ti}^{Cu_4Ti_3}$	$x_{Ti}^{Cu_2Ti}$	Reference
		Experimental data		
1165	-	0.4	0.333	[20]
–	0.290 ± 0.01	0.4	0.333	[24]
1151	–	0.429	0.333	[26]
1158 ± 3	–	0.42–0.43	0.333	[27]
		Calculated data		
1160	0.272	0.429	0.333	[47]
1158	0.287	0.429	0.333	P. p.

TABLE 2. *Continued*

$Cu_2Ti + Cu_4Ti_3 \Leftrightarrow Cu_3Ti_2$

T, K	$x_{Ti}^{Cu_2Ti}$	$x_{Ti}^{Cu_4Ti_3}$	$x_{Ti}^{Cu_3Ti_2}$	Reference
		Experimental data		
1158	0.333	–	0.4	[20]
>1143	0.333	0.429	0.4	[25]
1138	0.333	0.429	0.4	[26]
		Calculated data		
1148	0.333	0.429	0.400	[47]
1150	0.333	0.429	0.400	P. p.

$L + CuTi \Leftrightarrow Cu_4Ti_3$

T, K	x_{Ti}^{L}	x_{Ti}^{CuTi}	$x_{Ti}^{Cu_4Ti_3}$	Reference
		Experimental data		
1189	–	0.5	0.4	[18]
1208	–	0.5	0.4	[20]
–	0.375 ± 0.005	0.5	0.4	[24]
1191	–	0.48–0.52	0.429	[26]
1202 ± 4	–	0.50–0.52	0.42–0.43	[27]
1208 ± 5	–	–	0.429	[32]
		Calculated data		
1206	0.360	0.485	0.429	[47]
1189	0.347	0.490	0.429	P. p.

$L \Leftrightarrow CuTi$

T, K	x_{Ti}^{L}	Reference
	Experimental data	
1245	0.5	[18]
1278	0.5	[19]
1255	0.5	[20]
1257	0.5	[26]
1257 ± 5	0.5	[27]
1253 ± 5	0.5	[32]
	Calculated data	
1248	0.507	[47]
1251	0.505	P. p.

$L \Leftrightarrow CuTi + CuTi_2$

T, K	x_{Ti}^{L}	x_{Ti}^{CuTi}	$x_{Ti}^{CuTi_2}$	Reference
		Experimental data		
1227	0.57	0.5	0.667	[18]
1233	0.57	0.5	0.667	[20]
1233	0.57	0.48–0.52	0.67–0.7	[26]
1233 ± 3	0.43	0.5–0.52	0.67–0.7	[27]

TABLE 2. *Continued*

$L \Leftrightarrow CuTi + CuTi_2$

T, K	x_{Ti}^{L}	x_{Ti}^{CuTi}	$x_{Ti}^{CuTi_2}$	Reference
		Calculated data		
1242	0.564	0.517	0.667	[47]
1234	0.569	0.513	0.667	P. p.

$L \Leftrightarrow CuTi_2$

T, K	x_{Ti}^{L}	Reference
	Experimental data	
1288	0.667	[20]
1288	0.667	[26]
1283 ± 3	0.667	[27]
1285 ± 3	0.667	[33]
	Calculated data	
1282	0.667	P. p.

$L \Leftrightarrow CuTi_2 + (\beta Ti)$

T, K	x_{Ti}^{L}	$x_{Ti}^{(\beta Ti)}$	$x_{Ti}^{CuTi_2}$	Reference
		Experimental data		
1282	~0.69	–	0.667	[20]
1273	0.69	–	0.667	[26]
1276 ± 3	0.69	–	0.67–0.7	[27]
1275	–	0.840	0.667	[34]
		Calculated data		
1231	0.754	0.875	0.667	P. p.

$(\beta Ti) \Leftrightarrow CuTi_2 + (\alpha Ti)$

T, K	$x_{Ti}^{(\beta Ti)}$	$x_{Ti}^{CuTi_2}$	$x_{Ti}^{(\alpha Ti)}$	Reference
		Experimental data		
1049	0.93	0.667	0.9875	[17]
1071	0.945	0.667	0.984	[18]
1073	–	0.67–0.7	–	[26]
1073 ± 5	–	0.67–0.7	–	[27]
1053 ± 5	–	0.667	0.986	[29]
1073	0.944		0.984	[34]
		Calculated data		
1072	0.951	0.667	0.986	[47]
1065	0.953	0.667	0.984	P. p.

* Data of the present paper.

The liquidus and solidus of the (βTi)-phase at high temperatures remain the least understood sections of the phase diagram. The liquidus of the (βTi)-phase at 1400–1941 K has scarcely been analyzed. The ranges where the (αTi)- and (βTi)-phases exist below 1300 K (Fig. 4) were studied in [17, 18, 29, 34]. According to these data, the solubility of copper in the (βTi)-phase is many-fold higher than in the (αTi)-phase.

Thermodynamic Properties of the Phases. The experimental studies into the thermodynamic properties of liquid alloys of copper and titanium were analyzed in detail in [15].

All available experimental data on the thermodynamic properties of liquid alloys of this system indicate considerable negative deviations from the ideal behavior. According to [15], the minima of the integral mixing enthalpy shift toward titanium-rich alloys. The following temperature-dependence of the mixing enthalpy was established in [15]: the mixing enthalpy becomes less exothermic with increasing temperature. The thermodynamic properties of the melts of the system were described in [15] using an ideal associated-solution (IAS) model [42] with two associates: CuTi and $CuTi_2$.

The thermodynamic properties of the intermetallic compounds of the system were analyzed in [32, 43–45]. The data on the equilibrium pressure of hydrogen over alloy and hydride obtained within 673–823 K were used in [43] to calculate the free energies of formation of Cu_4Ti, CuTi, and $CuTi_2$. In [44], the enthalpy of formation of CuTi was determined by the calorimetric method. The enthalpies of formation of Cu_4Ti, Cu_4Ti_3, Cu_3Ti_2, CuTi, and $CuTi_2$ were analyzed in [45] by mixing calorimetry (in liquid aluminum). A quantitative differential thermal analysis was carried out in [32] to determine the mixing enthalpy of CuTi. Table 3 summarizes the results from a study into the thermodynamic properties of intermetallic compounds. All available data on the thermodynamic properties of the compounds have been taken into account in optimization.

TABLE 3. Thermodynamic Properties of the Intermetallic Compounds of the Cu–Ti System

Compound	T, K	$\Delta_f G$, J/mole	$\Delta_f H$, J/mole	$\Delta_f S$, J/(mole · K)	Reference
Cu_4Ti	298	–	–5530 ± 1070	–	[45]
	673	–4627	–	–	[43]
	723	–4694	–	–	
	773	–4789	–	–	
	823	–4501	–	–	
	298	–	–7346	–1.85	Calculated
	673	–6864			
	723	–6793			
	773	–6731			
	823	–6676			
Cu_2Ti	298		–9871	–	Calculated
Cu_3Ti_2	298	–	–9350 ± 1300	–	[45]
			–13927	–2.08	Calculated
Cu_4Ti_3	298		–9650 ± 880	–	[45]
			–14921	–2.32	Calculated
CuTi	298	–	–11120 ± 1720	–	[45]
		–	–9610 ± 370	–	[44]
	673	–9815	–	–	[43]
	723	–9875	–	–	
	773	–9715	–	–	
	823	–9835	–	–	
	298	–	–17534	–3.37	Calculated
	673	–16384			
	723	–16077			
	773	–15776			
	823	–15481			
$CuTi_2$	298	–	–8600 ± 1620	–	[45]
	773	–8750	–	–	[43]
	298		–24220	–8.5	Calculated
	773	–18778			

Compound	T, K	$\Delta_m H$, J/mole	$\Delta_m S$, J/(mole · K)	Reference
CuTi	1248	15800	12.7	[44]
	1250	18635	15.0	[32]
	1251	15895	12.64	Calculated

THERMODYNAMIC ASSESSMENT OF THE SYSTEM AND MODEL

The copper–titanium system was repeatedly subjected to thermodynamic assessment. The paper [46] was the first to obtain the phase diagram of the system theoretically. There, thermodynamic models were constructed just for three compounds: $Cu_{0.77}Ti_{0.23}$, CuTi, and $CuTi_2$. The thermodynamic assessments of the system performed up to 1994 are reviewed in [38]. What these assessments have in common is that no thermodynamic models of Cu_2Ti and Cu_3Ti_2 were constructed. The paper [47] was the first to do a rigorous thermodynamic assessment of the system with allowance for the currently adopted set of intermetallic compounds and the homogeneity regions of the phases Cu_4Ti and CuTi. However, the paper [47] disregarded the results obtained in [27, 32, 33, 35, 36] in studying the phase equilibria and in [15, 45, 48] in analyzing the thermodynamic properties of the phases. As a consequence, the melting of $CuTi_2$ is considered in [47] to be incongruent and the thermodynamic model of liquid alloys disregards the temperature dependence of the integral mixing enthalpy. Moreover, the thermodynamic models of solid solutions adopted in [47] indicate positive deviations from the ideal behavior, which contradicts the way the components of the system interact. All of this provided the basis for a new thermodynamic assessment of the system.

The thermodynamic description of the system performed here is based on the CALPHAD-method. We will use the following models to describe the temperature and concentration dependences of the Gibbs energy of the phases.

Liquid Phase. The temperature–concentration dependence of the free energy of a liquid alloy is described by the expression

$$G^{\mathrm{L}}(x_{\mathrm{Ti}},T) = (1-x_{\mathrm{Ti}})({}^{\circ}G^{\mathrm{L}}_{\mathrm{Cu}}(T) - H^{\mathrm{SER}}_{\mathrm{Cu}}) + x_{\mathrm{Ti}}({}^{\circ}G^{\mathrm{L}}_{\mathrm{Ti}}(T) - H^{\mathrm{SER}}_{\mathrm{Ti}}) + \\ + \mathrm{R}T((1-x_{\mathrm{Ti}})\ln(1-x_{\mathrm{Ti}}) + x_{\mathrm{Ti}}\ln(x_{\mathrm{Ti}})) + \Delta G^{\mathrm{ex,L}}(x_{\mathrm{Ti}},T), \quad (1)$$

where x_{Ti} is the mole fraction of titanium; ${}^{\circ}G^{\mathrm{L}}_{\mathrm{Cu}}(T) - H^{\mathrm{SER}}_{\mathrm{Cu}}$ and ${}^{\circ}G^{\mathrm{L}}_{\mathrm{Ti}}(T) - H^{\mathrm{SER}}_{\mathrm{Ti}}$ are the free energies of pure liquid copper and titanium [49]; and $\Delta G^{\mathrm{ex,L}}(x_{\mathrm{Ti}},T)$ is the excess Gibbs energy of the liquid alloy. In this expression, the sum of the first and second terms describes the free energy of a mechanical two-component mixture, the third term the free mixing energy of an ideal solution of the components, and the fourth term the excess free mixing energy of a melt. Here the excess free mixing energy of melts is described with the ideal-associated-solution model proposed in [15].

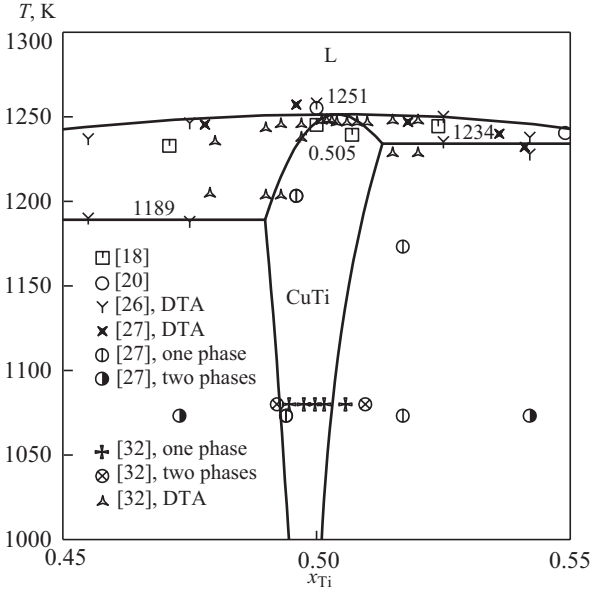

Fig. 3. Experimental and theoretical phase transformations for CuTi

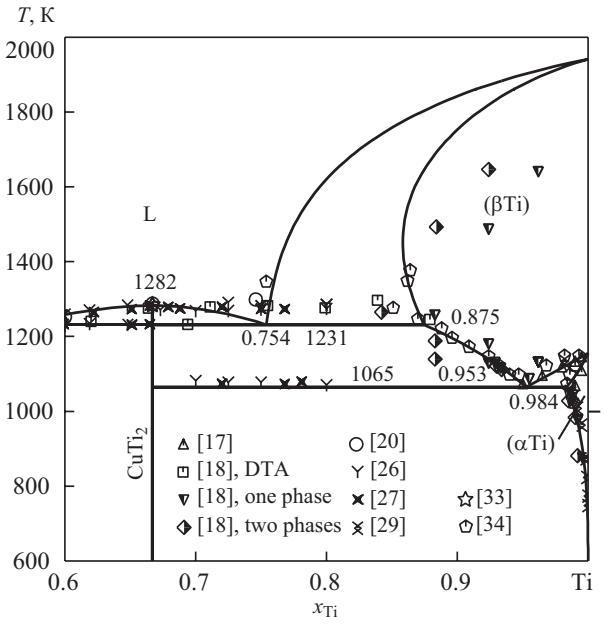

Fig. 4. Experimental and theoretical phase boundaries in the titanium-rich region of the phase diagram

Solid Solutions. The temperature–concentration dependence of the Gibbs energy of ϕ-solid solution is described by the expression

$$G^{\phi}(x_{\mathrm{Ti}},T) = (1-x_{\mathrm{Ti}})({}^{\circ}G^{\phi}_{\mathrm{Cu}} - H^{\mathrm{SER}}_{\mathrm{Cu}}) + x_{\mathrm{Ti}}({}^{\circ}G^{\phi}_{\mathrm{Ti}} - H^{\mathrm{SER}}_{\mathrm{Ti}}) + {+}\mathrm{R}T((1-x_{\mathrm{Ti}})\ln(1-x_{\mathrm{Ti}}) + \\ + x_{\mathrm{Ti}}\ln x_{\mathrm{Ti}}) + (1-x_{\mathrm{Ti}})x_{\mathrm{Ti}}\sum_{i=0}^{n}(1-2x_{\mathrm{Ti}})^{i}(A_i + B_i T), \tag{2}$$

where $({}^{\circ}G^{\phi}_{\mathrm{Cu}} - H^{\mathrm{SER}}_{\mathrm{Cu}})$ and $({}^{\circ}G^{\phi}_{\mathrm{Ti}} - H^{\mathrm{SER}}_{\mathrm{Ti}})$ are the Gibbs energies of pure copper and titanium with ϕ-structure [49]; and A_i and B_i are the model coefficients.

Intermetallic Compounds. To model the thermodynamic properties of the Cu_4Ti and CuTi phases with homogeneity region, we use the Compound Energy Formalism (CEF) [50–52]. The model with two sublattices $(\underline{\mathrm{Cu}}, \mathrm{Ti})_k : \mathrm{Cu}, \underline{\mathrm{Ti}})_l$ proposed in [47] is based on this formalism. The sublattice formula $(\underline{\mathrm{Cu}}, \mathrm{Ti})_4 : \mathrm{Cu}, \underline{\mathrm{Ti}})_1$ was used for Cu_4Ti and the formula $(\underline{\mathrm{Cu}}, \mathrm{Ti})_1 : \mathrm{Cu}, \underline{\mathrm{Ti}})_1$ for CuTi. In these formulas, the first sublattice is that of copper and the second sublattice is that of titanium (the main component is underlined.)

Within the CEF, the temperature–concentration dependence of the free energy per one mole of Cu_kTi_l is described by the following expression [51–53]:

$$G^{\mathrm{Cu}_k\mathrm{Ti}_l}(x_{\mathrm{Ti}},T) = {}^{1}y_{\mathrm{Cu}}{}^{2}y_{\mathrm{Cu}}G^{\mathrm{Cu}_k\mathrm{Ti}_l}_{\mathrm{Cu:Cu}} + {}^{1}y_{\mathrm{Cu}}{}^{2}y_{\mathrm{Ti}}G^{\mathrm{Cu}_k\mathrm{Ti}_l}_{\mathrm{Cu:Ti}} + {}^{1}y_{\mathrm{Ti}}{}^{2}y_{\mathrm{Cu}}G^{\mathrm{Cu}_k\mathrm{Ti}_l}_{\mathrm{Ti:Cu}} + {}^{1}y_{\mathrm{Ti}}{}^{2}y_{\mathrm{Ti}}G^{\mathrm{Cu}_k\mathrm{Ti}_l}_{\mathrm{Ti:Ti}} + \\ + \mathrm{R}T\left[\frac{k}{k+l}({}^{1}y_{\mathrm{Cu}}\ln{}^{1}y_{\mathrm{Cu}} + {}^{1}y_{\mathrm{Ti}}\ln{}^{1}y_{\mathrm{Ti}}) + \frac{l}{k+l}({}^{2}y_{\mathrm{Cu}}\ln{}^{2}y_{\mathrm{Cu}} + {}^{2}y_{\mathrm{Ti}}\ln{}^{2}y_{\mathrm{Ti}})\right] + {}^{1}y_{\mathrm{Cu}}{}^{1}y_{\mathrm{Ti}}\left[{}^{2}y_{\mathrm{Cu}}L^{\mathrm{Cu}_k\mathrm{Ti}_l}_{\mathrm{Cu,Ti:Cu}} + \right. \\ \left. + {}^{2}y_{\mathrm{Ti}}L^{\mathrm{Cu}_k\mathrm{Ti}_l}_{\mathrm{Cu,Ti:Ti}}\right] + {}^{2}y_{\mathrm{Cu}}{}^{2}y_{\mathrm{Ti}}\left[{}^{1}y_{\mathrm{Cu}}L^{\mathrm{Cu}_k\mathrm{Ti}_l}_{\mathrm{Cu:Cu,Ti}} + {}^{1}y_{\mathrm{Ti}}L^{\mathrm{Cu}_k\mathrm{Ti}_l}_{\mathrm{Ti:Cu,Ti}}\right], \tag{3}$$

where ${}^{s}y_{\mathrm{Cu}}$ and ${}^{s}y_{\mathrm{Ti}}$ are the fractions of the components in the sublattice s; $G^{\mathrm{Cu}_k\mathrm{Ti}_l}_{\mathrm{Cu:Cu}}$, $G^{\mathrm{Cu}_k\mathrm{Ti}_l}_{\mathrm{Cu:Ti}}$, $G^{\mathrm{Cu}_k\mathrm{Ti}_l}_{\mathrm{Ti:Cu}}$, and $G^{\mathrm{Cu}_k\mathrm{Ti}_l}_{\mathrm{Ti:Ti}}$ are the free energies of hypothetical compounds with a similar structure in which each of the sublattices is occupied by atoms of the components indicated by the subscript; $L^{\mathrm{Cu}_k\mathrm{Ti}_l}_{\mathrm{Cu,Ti:Cu}}$, $L^{\mathrm{Cu}_k\mathrm{Ti}_l}_{\mathrm{Cu,Ti:Ti}}$ $L^{\mathrm{Cu}_k\mathrm{Ti}_l}_{\mathrm{Cu:Cu,Ti}}$, and $L^{\mathrm{Cu}_k\mathrm{Ti}_l}_{\mathrm{Ti:Cu,Ti}}$ are

parameters characterizing the interaction of the components in sublattices. The fractions of Cu and Ti in the sublattice *s* are given by

$$ {}^{s}y_{\mathrm{Cu}} = \frac{{}^{s}n_{\mathrm{Cu}}}{{}^{s}N}; {}^{s}y_{\mathrm{Ti}} = \frac{{}^{s}n_{\mathrm{Ti}}}{{}^{s}N}, $$

where ${}^{s}n_{\mathrm{Cu}}$ and ${}^{s}n_{\mathrm{Ti}}$ are the number of sites occupied by atoms of the components in the sublattice; ${}^{s}N$ is the total number of sites in the sublattice. The mole fraction of the components are related to the fractions of the components in the sublattices by

$$ x_{\mathrm{Cu}} = \frac{\sum_{s=1}^{2} {}^{s}N\,{}^{s}y_{\mathrm{Cu}}}{\sum_{s} {}^{s}N}, \; x_{\mathrm{Ti}} = \frac{\sum_{s=1}^{2} {}^{s}N\,{}^{s}y_{\mathrm{Ti}}}{\sum_{s} {}^{s}N}. $$

For the $\mathrm{Cu}_k\mathrm{Ti}_l$ compound with a narrow homogeneity range, the free energies of the hypothetical compounds $G^{\mathrm{Cu}_k\mathrm{Ti}_l}_{\mathrm{Cu:Cu}}$, $G^{\mathrm{Cu}_k\mathrm{Ti}_l}_{\mathrm{Cu:Ti}}$, $G^{\mathrm{Cu}_k\mathrm{Ti}_l}_{\mathrm{Ti:Cu}}$, and $G^{\mathrm{Cu}_k\mathrm{Ti}_l}_{\mathrm{Ti:Ti}}$ are described by the following expressions [53]:

$$ G^{\mathrm{Cu}_k\mathrm{Ti}_l}_{\mathrm{Cu:Cu}} = [({}^{\circ}G^{\mathrm{SER}}_{\mathrm{Cu}} - H^{\mathrm{SER}}_{\mathrm{Cu}}) + F], \tag{4} $$

$$ G^{\mathrm{Cu}_k\mathrm{Ti}_l}_{\mathrm{Cu:Ti}} = \frac{k}{k+l}({}^{\circ}G^{\mathrm{SER}}_{\mathrm{Cu}} - H^{\mathrm{SER}}_{\mathrm{Cu}}) + \frac{l}{k+l}({}^{\circ}G^{\mathrm{SER}}_{\mathrm{Ti}} - H^{\mathrm{SER}}_{\mathrm{Ti}}) + \Delta_f H^{\mathrm{Cu}_k\mathrm{Ti}_l} - \Delta_f S^{\mathrm{Cu}_k\mathrm{Ti}_l} T, \tag{5} $$

$$ G^{\mathrm{Cu}_k\mathrm{Ti}_l}_{\mathrm{Ti:Ti}} = [({}^{\circ}G^{\mathrm{SER}}_{\mathrm{Ti}} - H^{\mathrm{SER}}_{\mathrm{Ti}}) + F], \tag{6} $$

$$ G^{\mathrm{Cu}_k\mathrm{Ti}_l}_{\mathrm{Ti:Cu}} = G^{\mathrm{Cu}_k\mathrm{Ti}_l}_{\mathrm{Cu:Cu}} + G^{\mathrm{A}_k\mathrm{B}_l}_{\mathrm{Ti:Ti}} - G^{\mathrm{A}_k\mathrm{B}_l}_{\mathrm{Cu:Ti}}, \tag{7} $$

where $\Delta_f H^{\mathrm{Cu}_k\mathrm{Ti}_l}$ and $\Delta_f S^{\mathrm{Cu}_k\mathrm{Ti}_l}$ are the enthalpy and entropy of formation; *F* is a parameter that accounts for the free energy of formation of a compound with antisite atoms and may depend on temperature. The parameters characterizing the interaction of the components in sublattices are expressed as Redlich–Kister polynomials [53]:

$$ L^{\mathrm{Cu}_k\mathrm{Ti}_l}_{\mathrm{Cu,Ti:Cu}} = \sum_{v=0}^{n} ({}^{1}A^{\mathrm{v}} + {}^{1}B^{\mathrm{v}}T)({}^{1}y_{\mathrm{Cu}} - {}^{1}y_{\mathrm{Ti}})^{\mathrm{v}}, \tag{8} $$

$$ L^{\mathrm{Cu}_k\mathrm{Ti}_l}_{\mathrm{Cu,Ti:Ti}} = \sum_{v=0}^{n} ({}^{1}A^{\mathrm{v}} + {}^{1}B^{\mathrm{v}}T)({}^{1}y_{\mathrm{Cu}} - {}^{1}y_{\mathrm{Ti}})^{\mathrm{v}}, \tag{9} $$

$$ L^{\mathrm{Cu}_k\mathrm{Ti}_l}_{\mathrm{Cu:Cu,Ti}} = \sum_{v=0}^{n} ({}^{2}A^{\mathrm{v}} + {}^{2}B^{\mathrm{v}}T)({}^{2}y_{\mathrm{Cu}} - {}^{2}y_{\mathrm{Ti}})^{\mathrm{v}}, \tag{10} $$

$$ L^{\mathrm{Cu}_k\mathrm{Ti}_l}_{\mathrm{Ti:Cu,Ti}} = \sum_{v=0}^{n} ({}^{2}A^{\mathrm{v}} + {}^{2}B^{\mathrm{v}}T)({}^{2}y_{\mathrm{Cu}} - {}^{2}y_{\mathrm{Ti}})^{\mathrm{v}}, \tag{11} $$

where, ${}^{s}A^{v}$ and ${}^{s}B^{v}$ are parameters describing the excess Gibbs energy in the sublattice s; *v* is the degree of the Redlich–Kister polynomial. We can use expression (3) with ${}^{1}y_{\mathrm{Cu}} = 1$, ${}^{1}y_{\mathrm{Ti}} = 0$, ${}^{2}y_{\mathrm{Cu}} = 0$, and ${}^{2}y_{\mathrm{Ti}} = 1$ to derive an expression for the Gibbs energy of a $\mathrm{Cu}_k\mathrm{Ti}_l$ intermetallic compound that does not have homogeneity ranges. For compounds of such type, the temperature dependence of the Gibbs energy per one mole is described by the model

$$ G^{\mathrm{Cu}_k\mathrm{Ti}_l}(T) = \frac{k}{k+l}({}^{\circ}G^{\mathrm{SER}}_{\mathrm{Cu}} - H^{\mathrm{SER}}_{\mathrm{Cu}}) + \frac{l}{k+l}({}^{\circ}G^{\mathrm{SER}}_{\mathrm{Ti}} - H^{\mathrm{SER}}_{\mathrm{Ti}}) + \Delta_f H^{\mathrm{Cu}_k\mathrm{Ti}_l} - \Delta_f S^{\mathrm{Cu}_k\mathrm{Ti}_l} T, \tag{12} $$

where $\Delta_f H^{\mathrm{Cu}_k\mathrm{Ti}_l}$ and $\Delta_f S^{\mathrm{Cu}_k\mathrm{Ti}_l}$ are the enthalpy and entropy of formation. A similar model was used to assess the thermodynamic properties of $\mathrm{Cu_2Ti}$, $\mathrm{Cu_3Ti_2}$, $\mathrm{Cu_4Ti_3}$, and $\mathrm{CuTi_2}$.

Optimization of Model Parameters. The model parameters for the phases have been optimized in three stages. The first stage employs the data [18, 20, 24–27, 31–33] on the temperatures of invariant transformations and compositions of the phases and the data [32, 43–45] on the thermodynamic properties of the phases. At this stage,

parameters A_0 and B_0 are chosen for thermodynamic models of terminal solid solutions, and the Gibbs energy of all intermetallic compounds is described by expression (12).

At the second stage, the data [20, 26, 27, 32] on the liquidus position and on the concentration ranges of the (Cu)-phase [20–23, 36] and the (αTi)- and (βTi)-phases [17, 18, 29, 34] are added to the optimization set and the thermodynamic models of solid solutions are refined. The parameters A_0 and B_0 are used to describe the thermodynamic properties of the (Cu)-phase. For the (αTi)-phase, the parameter A_0 appeared sufficient. The properties of the (βTi)-phase are described using the parameters A_0, B_0, and A_1. It was established that a model with one parameter corresponding to the enthalpy of formation of $\Delta_f H^{CuTi_2}$ can be used to describe the thermodynamic properties of Cu_2Ti.

At the third stage, the optimized data set is supplemented with experimental data on the homogeneity range of Cu_4Ti [27, 28, 31] and CuTi [27, 32]. The thermodynamic properties of the Cu_4Ti and CuTi phases are described by expression (3). The values of $\Delta_f H^{Cu_kTi_l}$ and $\Delta_f S^{Cu_kTi_l}$ obtained at the second stage are used as starting values for the corresponding parameters in (4)–(7). It is assumed that F = 5000 J/mole [47]. The optimized model parameters are summarized in Table 4. The calculated coordinates of invariant equilibria are given in Table 2. The calculated phase diagram of the system is plotted in Fig. 5.

RESULTS AND DISCUSSION

Figures 1–4 demonstrate satisfactory agreement between calculated results and the majority of experimental data on phase equilibria in the system. In the range of copper-rich alloys (Fig. 1), the theoretical results are in the best agreement with the data from [20–23, 26, 27, 31, 36]. The calculations confirm the peritectic formation of Cu_4Ti established in [18, 19, 24, 26, 27, 31]. The calculated homogeneity range of Cu_4Ti (Fig. 1) is in good agreement with the experimental data from [27, 28, 31]. Comparing the results of modeling and studying the thermodynamic properties of this intermetallic compound (Table 3) reveal good agreement between the calculated and experimental values [43, 45] for $\Delta_f G^{Cu_4Ti}$ and $\Delta_f H^{Cu_4Ti}$.

Satisfactory agreement is also achieved in describing the liquidus in the middle region of the phase diagram (Fig. 2). The calculated parameters of the phase equilibria for intermetallic compounds are in good agreement with the data from [20, 24–27, 32] (Table 2). The calculated temperature of the reaction L+ CuTi ⇔Cu_4Ti_3 is 1189 K, which agrees well with the data from [18, 26]. The calculated homogeneity range of CuTi (Fig. 3) is conformed by the experimental data [32]. The melting point of this compound is 1253 ± 5 K according to the DTA [32] and is 1251 K according to the calculation for x_{Ti} = 0.505. Also, there is good agreement between the experimental [32, 44] and calculated (Table 3) values of the melting enthalpy for $\Delta_m H^{CuTi}$. No quantitative agreement is achieved between experiment [43–45] and theory in modeling the thermodynamic properties of other intermetallic compounds in this region of the phase diagram. Attempts to improve their description deteriorated the thermal stability of the compounds and decreased the temperatures of invariant transformations and liquidus. Therefore, we preferred the data from [20, 26, 27, 32, 33], which are in satisfactory agreement with each other, in describing the central region of the phase diagram, while the data from [43–45] were used in optimization with a low weight coefficient.

The calculated results confirm that $CuTi_2$ forms congruently (Fig. 4), as established in [20, 26, 27, 33]. Table 2 indicates that the calculated temperature of formation of this compound is in good agreement with the results obtained in [20, 26, 27, 33]. The calculated temperature of the eutectic reaction L ⇔ $CuTi_2$ + (βTi) is 1231 K (Table 2), which is close to that reported in [20, 26, 27, 34]. Below 1400 K, the calculated results and experimental data for the liquidus [18, 20, 26, 27, 34] and solidus [18, 34] of the (βTi)-phase are in good agreement. Above 1400 K, just qualitative agreement with [18] is achieved. The calculated phase boundary (βTi)/($CuTi_2$ + (βTi)) fits well the data from [18, 34]. The calculated phase boundaries (βTi)/((αTi) + (βTi)) and (αTi)/((αTi) + (βTi)) are in good agreement with the experimental data from [17, 34]. Good agreement is achieved

TABLE 4. Model Parameters for the Gibbs Energy (J/mole) of the Phases in the Cu–Ti System

Phase	Parameters			
	ΔH_{CuTi}	ΔS_{CuTi}	$\Delta H_{\mathrm{CuTi_2}}$	$\Delta S_{\mathrm{CuTi_2}}$
L	–29500	–10	–67500	–23.7

$$\Delta G^{\mathrm{ex},\phi}(x_{\mathrm{Ti}},T) = (1-x_{\mathrm{Ti}})x_{\mathrm{Ti}}\sum_{i=0}^{n}(1-2x_{\mathrm{Ti}})^{i}(A_i + B_iT)$$

Phase	i	A_i	B_i
(Cu)	0	–14326	2.9
(αTi)	0	–10000	–
(βTi)	0	–10881.2	–9.66
	1	2341.6	–

Phase	Parameters	
	$\Delta_f H^{\mathrm{Cu_4Ti}}$	$\Delta_f S^{\mathrm{Cu_4Ti}}$
Cu_4Ti	–7603	–3.12

$$\mathrm{L}^{\mathrm{Cu_4Ti}}_{\mathrm{Cu,Ti:Cu}} = \mathrm{L}^{\mathrm{Cu_4Ti}}_{\mathrm{Cu,Ti:Ti}} = {}^{1}A^{0} + {}^{1}B^{0}T$$

Phase	${}^{1}A^{0}$	${}^{1}B^{0}$
Cu_4Ti	–35823	17.342

$$\mathrm{L}^{\mathrm{Cu_4Ti}}_{\mathrm{Cu:Cu,Ti}} = \mathrm{L}^{\mathrm{Cu_4Ti}}_{\mathrm{Ti:Cu,Ti}} = {}^{2}A^{0} + {}^{2}B^{0}T$$

Phase	${}^{2}A^{0}$	${}^{2}B^{0}$
Cu_4Ti	–4009.8	–2.726

$$\Delta_f G^{\mathrm{Cu}_k\mathrm{Ti}_l}(T) = \Delta_f H^{\mathrm{Cu}_k\mathrm{Ti}_l} - T\Delta_f S^{\mathrm{Cu}_k\mathrm{Ti}_l}$$

Phase	$\Delta_f H^{\mathrm{Cu}_k\mathrm{Ti}_l}$	$\Delta_f S^{\mathrm{Cu}_k\mathrm{Ti}_l}$
Cu_2Ti	–9871	–
Cu_3Ti_2	–13927	–2.078
Cu_4Ti_3	–14920.7	–2.321

Phase	Parameters	
	$\Delta_f H^{\mathrm{CuTi}}$	$\Delta_f S^{\mathrm{CuTi}}$
CuTi	–17534	–3,372

$$\mathrm{L}^{\mathrm{CuTi}}_{\mathrm{Cu,Ti:Cu}} = \mathrm{L}^{\mathrm{CuTi}}_{\mathrm{Cu,Ti:Ti}} = {}^{1}A^{0} + {}^{1}B^{0}T$$

Phase	${}^{1}A^{0}$	${}^{1}B^{0}$
CuTi	1000	–

$$\mathrm{L}^{\mathrm{CuTi}}_{\mathrm{Cu:Cu,Ti}} = \mathrm{L}^{\mathrm{CuTi}}_{\mathrm{Ti:Cu,Ti}} = {}^{2}A^{0} + {}^{2}B^{0}T$$

Phase	${}^{2}A^{0}$	${}^{2}B^{0}$
CuTi	10000	–

$$\Delta_f G^{\mathrm{Cu}_k\mathrm{Ti}_l}(T) = \Delta_f H^{\mathrm{Cu}_k\mathrm{Ti}_l} - T\Delta_f S^{\mathrm{Cu}_k\mathrm{Ti}_l}$$

Phase	$\Delta_f H^{\mathrm{CuTi_2}}$	$\Delta_f S^{\mathrm{CuTi_2}}$
$CuTi_2$	–24220	–8.5

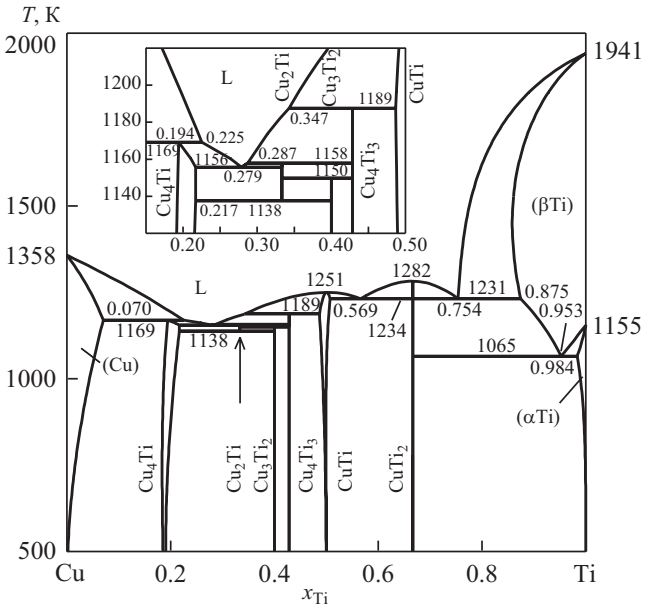

Fig. 5. Calculated phase diagram of the copper–titanium system

in describing the solubility of copper in (αTi) [18, 29, 34]. The calculated temperature of the reaction (βTi) ⇔ $CuTi_2$ + (αTi) is 1065 K, which agrees well with the data [17, 18, 26, 27, 29, 34].

The calculated phase diagram of the Cu-Ti system features convex liquidus and solidus of the (βTi)-phase. As follows from [47, 54], these lines are less curved. In our opinion, the calculated phase boundaries for the liquid and (βTi) phases are justified enough because the associated thermodynamic models allow correct description of the adjacent regions L + $CuTi_2$, (βTi) + $CuTi_2$, and (αTi) + (βTi) and the phase boundaries (βTi)/($CuTi_2$ + (βTi)), (βTi)/((αTi) + (βTi)), L/(L + (βTi)), and (βTi)/(L + (βTi)). A model of the (βTi)-phase, which indicates positive deviations of its thermodynamic mixing functions from the ideal behavior was used in [47] to describe the titanium-rich region of the phase diagram, which is similar to that presented in [54]. As mentioned above, this behavior of the model is inconsistent with the way the components of the system interact. It is obvious that a conclusion on the concentration dependence of the liquidus and solidus of the (βTi)-phases can be drawn only after special experimental research.

An important feature of this thermodynamic assessment of the system is the use of the IAS model for the thermodynamic properties of liquid alloys [15]. As shown in [15], this model successfully describes the thermodynamic properties of liquid alloys over wide ranges of temperatures and concentrations, and extrapolating it to the supercooling range makes it possible to reproduce well the thermodynamic properties of the amorphous alloys studied in [45]. As will be shown in the next papers, this is a decisive factor that allows correct description of the phase transformations for the liquid phase in the Cu–Ti–Zr system at temperatures above 1000 K and modeling of metastable transformations involving it.

REFERENCES

1. A. Inoue, "Stabilization of metallic supercooled liquid and bulk amorphous alloys," *Acta Mater.*, **48**, 279–306 (2000).
2. Y. Zhang, D. Q. Zhao, M. X. Pan, and W. H. Wang, "Glass forming properties of Zr-based bulk metallic alloys," *J. Non-Crystalline Solids*, **315**, 206–210 (2003).
3. E. Ence and H. Margolin, "A study of the Ti–Cu–Zr system and the structure of Ti_2Cu," *Trans. Metal. Soc. AIME*, **221**, 320–322 (1961).

4. C. G. Woychik and T. B. Massalski, “Phase diagram relationships in the system copper–titanium–zirconium,” *Z. Metallkd.*, **79**, No. 3, 149–153 (1988).
5. V. N. Chebotnikov and V. V. Molokanov, “Structure and properties of alloys of the Ti_2Cu–Zr_2Cu section of the Ti–Zr–Cu system in amorphous and crystalline states,” *Izv. AN SSSR, Neorg. Mater.*, **26**, No. 5, 960–964 (1990).
6. Yu. K. Kovneristyi and A. G. Pashkovskaya, “Bulk amorphization of alloys of the Ti–Cu–Zr system which includes intermetallic compounds,” in: *Amorphization (Glass Formation) of Metallic Materials* [in Russian], Inst. Metallurgii RAN, Moscow (1992), pp. 153–157.
7. A. M. Storchak-Fedyuk, V. M. Petyukh, and L. V. Artyukh, “Study of cast alloys of the Cu–Ti–Zr system,” in: *Modern Problems of Materials Science, Ser. Physical and Chemical Fundamentals of Powder Technology* [in Russian], Kiev (2007), pp. 22–26.
8. A. Inoue, W. Zhang, T. Zhang, and K. Kurosaka, “High-strength Cu-based bulk glassy alloys in Cu–Zr–Ti and Cu–Hf–Ti ternary systems,” *Acta Mater.*, **49**, No. 14, 2645–2652 (2001).
9. T. Shindo, Y. Waseda, and A. Inoue, “Prediction of critical compositions for bulk glass formation in La-based, Cu-based and Zr-based ternary alloys,” *Mater. Trans.*, JIM, **44**, No. 3, 351–357 (2003).
10. Q. S. Zhang, H. F. Zhang, Y. F. Deng, et al., “Bulk metallic glass formation of Cu–Zr–Ti–Sn alloys,” *Scr. Mater.*, **49**, No. 4, 273–278 (2003).
11. R. Arroyave, T. W. Eagar, and L. Kaufman, “Thermodynamic assessment of the Cu–Ti–Zr system,” *J. Alloys Compd.*, **351**, No. 1-2, 158–170 (2003).
12. T. Velikanova and M. A. Turchanin, “Cu–Ti–Zr,” in: *Ternary Alloy Systems. Phase Diagrams, Crystallographic and Thermodynamic Dat*a, G. Effenberg and S. Ilyenko (eds.), Vol. 11C3, Springer-Verlag, Germany, Berlin, Heidelberg (2006), pp. 436–464.
13. A. R. Abdulov, M. A. Turchanin, P. G. Agraval, and A. A. Solorev, “Mixing enthalpy of liquid alloys of the Cu–Ti–Zr system,” *Metally*, No. 1, 28–34 (2007).
14. U. Thiedermann, M. Rosner-Kuhn, K. Drewes, et al., “Mixing enthalpy measurements of liquid Ti–Zr, Fe–Ti–Zr, and Fe–Ni–Zr alloys,” *J. Steel Research*, **70**, No. 1, 3–8 (1999).
15. M. A. Turchanin, P. G. Agraval, A. N. Fesenko, and A. R. Abdulov, “Thermodynamics of liquid alloys and metastable phase transformations in the copper-titanium system,” *Powder Metall. Met. Ceram.*, **44**, No. 5-6, 259–270 (2005).
16. A. A. Turchanin, I. A. Tomilin, M. A. Turchanin, et al., “Enthalpies of formation of liquid and amorphous Zr–Cu alloys,” *J. Non-Crystalline Solids*, **250-252**, 582–585 (1999).
17. A. D. McQuillan, “The application of hydrogen equilibrium-pressure measurements to the investigation of titanium alloy systems,” *J. Ins. Metals.*, **79**, 73–88 (1951).
18. A. Joukainen, N. J. Grant, and C. F. Floe, “Titanium–copper binary phase diagram,” *J. Metals*, **4**, 766–770 (1952).
19. E. Raub, P. Walter, and H. Engel, “Alloys of titanium with copper, silver and gold,” *Z. Metallkd.*, **43**, 112–118 (1952).
20. W. Trzebiatowski, J. Berak, and T. Romotowski, “The copper–titanium system,” *Roczniki Chemii*, **27**, 426–437 (1953).
21. V. N. Vigdorovich, A. N. Krestovnikov, and M. V. Mal’tsev, “Microhardness investigation of solid solutions of ternary systems,” *Izvest. Akad. Nauk SSSR. Otdel. Tekh. Nauk*, No. 3, 110–113 (1958).
22. M. J. Saarivirta and H. S. Cannon, “Copper–titanium alloys,” *Metal Progress*, **76**, No. 2, 81–84 (1959).
23. K. P. Kalinin and M. Z. Spiridonov, “Studying the properties of copper–titanium alloys,” *Tr. Gos. Nauchn.-Issled. Proektn. Inst. Obrab. Tsvetn. Metal.*, **18**, 46–57 (1960).
24. P. Pietrokowsky and J. R. Maticich, “Use of the electron microprobe analyzer in the study of binary metal alloy systems,” in: *Proc. 3rd Int. Symp. X-Ray Opt. X-Ray Microanalysis*, Stanford (1963), pp. 591–602.
25. K. Schubert, “About titanium–copper and titanium–silver systems,” *Z. Metallkd.*, **56**, No. 3, 197–199 (1965).

26. V. N. Eremenko, Yu. I. Buyanov, and S. B. Prima, "Phase diagram of the system titanium–copper," *Powder Metall. Met. Ceram.*, **5**, No. 6, 494–502 (1966).
27. V. N. Eremenko, Yu. I. Buyanov, and N. M. Panchenko, "Polythermal and isothermal sections of the system titanium–copper–silver," *Powder Metall. Met. Ceram.*, **9**, No. 5, 410–414 (1970).
28. R. C. Ecob, J. V. Bee, and B. Ralph, "The structure of the β-phase in dilute copper-titanium alloys," *Physica Stat. Sol. A*, **52**, No. 1, 201–210 (1979).
29. G. Vigier, J. M. Pelletier, and J. Merlin, "Determination of copper solubility in titanium and study of titanium–copper solid solution stability by thermoelectric power measurements," *J. Less-Common Met.*, **64**, No. 2, 175–183 (1979).
30. K. Nagata and S. Nishikawa, "Aging and reversion phenomena of copper–titanium alloy," in: *Report of the Institute of Industrial Science*, University of Tokyo, **29**, No. 4, p. 40 (1981).
31. J.-Y. Brun, S.-J-H. Thibault, and C.-H. Allibert, "Cu–Ti and Cu–Ti–Al solid state phase equilibria in the copper-rich region," *Z. Metallkd.*, **74**, No. 8, 525–529 (1983).
32. V. N. Eremenko, R. N. Mogilevskii, V. M. Sergeenkova, and V. M. Petyuukh, "Melting heat and homogeneity range of TiCu intermetallic compound," *Izv. AN SSSR, Metally*, No. 6, 171–173 (1988).
33. S. P. Alisova, N. V. Lutskaya, A. N. Kobylkin, and P. B. Budberg, "The TiFe–Ti_2Cu section of the Ti–Fe–Cu system. Conditions for the formation of Ti_2Cu," *Metally*, No. 5, 170–172 (1994).
34. T. Yamane, S. Nakajima, H. Araki, et al., "Partial phase diagrams of the titanium-rich region of the Ti–Cu system under high pressure," *J. Mater. Sci. Lett.*, **13**, No. 3, 162–164 (1994).
35. V. E. Oliker, A. A. Mamonova, and T. I. Shaposhnikova, "Structure and phase composition of the Ti–Cu diffusion zone," *Powder Metall. Met. Ceram.*, **35**, No. 3-4, 173–175 (1996).
36. S. Nagarjuna and D. S. Sarma, "On the variation of lattice parameter of Cu solid solution with solute content in Cu–Ti alloys," *Scr. Mater.*, **41**, No. 4, 359–363 (1999).
37. P. Canale and C. Servant, "Thermodynamic assessment of the Cu–Ti system taking into account the new stable phase $CuTi_3$," *Z. Metallkd.*, **93**, 273–276 (2002).
38. J. L. Murray, "Cu–Ti (copper–titanium)," in: *Phase Diagrams of Binary Copper Alloys*, ASM, Ohio (1994), pp. 447–460.
39. N. Karlsson, "An x-ray study of the phases in the copper–titanium system," *J. Inst. Met.*, **79**, 391–405 (1951).
40. M. H. Mueller and H. W. Knott, "The Crystal Structures of Ti_2Cu, Ti_2Ni, Ti_4Ni_2O, and Ti_4Cu_2O," *Trans. Metall. Soc. AIME*, **227**, 674–678 (1963).
41. G. Lutjerung and S. Weissmann, "Mechanical properties and structure of age-hardened Ti–Cu alloys," *Metal. Trans.*, **1**, No. 6, 1641–1649 (1970).
42. M. A. Turchanin, I. V. Belokonenko, and P. G. Agraval, "Applying the ideal associated-solution theory to the description of the temperature–concentration dependence of the thermodynamic properties of binary melts," *Rasplavy*, No. 1, 58–69 (2001).
43. M. Arita, R. Kinaka, and M. Someno, "Application of the metal-hydrogen equilibration for determining thermodynamic properties in the titanium-copper system," *Met. Trans. A*, **10**, No. 5, 529–534 (1979).
44. O. I. Kleppa and S. Watanabe, "Thermochemistry of alloys of transition metals. Part III. Copper–silver, –titanium, –zirconium and –hafnium at 1373 K," *Met. Trans. B*, **13**, No. 1, 391–401 (1982).
45. C. Colinet, A. Pasturel, and K. H. J. Buschow, "Enthalpies of formation of Ti–Cu intermetallic and amorphous phases," *J. All. Comp.*, **247**, 15–19 (1997).
46. L. Kaufman, "Coupled phase diagrams and thermochemical data for transition metal binary systems-III," *CALPHAD*, **2**, No. 2, 117–146 (1978).
47. H. Kumar, I. Ansara, P. Wollants, and L. Delaey, "Thermodynamic optimization of the Cu–Ti system," *Z. Metallkd.*, **87**, No. 8, 666–672 (1996).
48. M. A. Turchanin and S. V. Porokhnya, "Enthalpy of formation of liquid alloys of copper with titanium and zirconium," *Rasplavy*, No. 5, 29–32 (1995).

49. A. T. Dinsdale, “SGTE data for pure elements,” CALPHAD, **15**, No. 4, 317–425 (1991).
50. J.-O. Andersson, A. F. Guillermet, M. Hillert, et al., “A compound-energy model of ordering in a phase with sites of different coordination numbers,” *Acta Metall.*, **34**, 437–445 (1986).
51. N. Saunders and A. P. Miodownik, CALPHAD (Calculation of Phase Diagrams), in: *Comprehensive Guide, Vol. 1*, Pergamon Materials Series (1998), p. 496.
52. M. Hillert, “The compound energy formalism,” *J. Alloys Compd.*, **320**, 161–176 (2001).
53. I. Ansara, T. G. Chart, A. Fernandez Guillermet, et. al., “Group 2: Alloy system I thermodynamic modeling of selected topologically close-packed intermetallic compounds,” *CALPHAD*, **21**, No. 2, 171–218 (1997).
54. T. B. Massalski, H. Okamoto, P. R. Subramanian, and L. Kacprzak (eds.), *Binary Alloys Phase Diagrams*, 2nd ed., ASM International, Ohio (1990), p. 3589.